THE ASTROPHYSICAL JOURNAL, 494:783–791, 1998 February 20

THE INFRARED DEVELOPMENT OF V705 CASSIOPEIAE

C. G. MASON AND R. D. GEHRZ
Astronomy Department, School of Physics and Astronomy, 116 Church Street SE, University of Minnesota, Minneapolis, MN 55455
CHARLES E. WOODWARD[1] AND J. B. SMILOWITZ[2]
Wyoming Infrared Observatory, Department of Physics and Astronomy, University of Wyoming, Laramie, WY 82071-3905
AND
T. L. HAYWARD AND J. R. HOUCK
Center for Radio Physics and Space Research, 226 Space Sciences Building, Cornell University, Ithaca, NY 14853
Received 1997 March 6; accepted 1997 September 30

ABSTRACT

We report 1.2–18.5 μm spectrophotometric measurements of the CO nova V705 Cassiopeiae (Nova Cas 1993). Observations were made over a 2.5 yr period between 7.1 and 929.4 days past outburst. This time frame was marked by all major phases of nova evolution. An optically thick, carbon dust shell formed by day 70.9. Later evolutionary stages of the dust shell are modeled using a combination of emission from carbon, silicate, and hydrocarbon grains. Using this model, we estimate carbon, silicate, and gas abundances in addition to several other calculable physical parameters.

Subject headings: circumstellar matter — dust, extinction — infrared: stars — novae, cataclysmic variables — stars: individual (V705 Cassiopeiae)

1. INTRODUCTION

V705 Cassiopeiae (Nova Cass 1993) was discovered on 1993 December 7 UT by K. Kanatsu (Kanatsu 1993) at a visible magnitude of 6.5. On 1993 December 12 UT, the nova flared to about 5.3 mag and quickly returned to preflare magnitude. Within 64 days, V705 Cas had declined 2 mag in the visible, classifying it as a moderately fast nova (Payne-Gaposchkin 1964). By day 100, the nova had plummeted nearly 6.5 mag in the visible from its methodical exponential decay, signaling the formation of an optically thick (at $V = 0.55$ μm) dust shell. V705 Cas is one of many recent novae to have formed dust in their ejecta (see the review articles by Bode & Evans 1989; Gehrz 1988, 1990, 1993, 1995; Gehrz, Truran, & Williams 1991). The severity of the visible decline observed in this object categorizes it as a DQ Her–type nova.

Infrared (IR) observations have helped to define the physical properties and mineral composition of grains formed in nova ejecta. Most dust-forming novae condense amorphous carbon that produces a featureless gray body or blackbody spectral energy distribution (SED) from 1 to 25 μm. These novae result from the thermonuclear runaways (TNRs) on low-mass, CO white dwarfs (WDs) (see Gehrz et al. 1995b) and are typified by NQ Vul (Ney & Hatfield 1978) and LW Ser (Gehrz et al. 1980). A growing number of novae are providing evidence that other types of common astrophysical dust can grow in ejecta. V1370 Aql (Bode et al. 1984; Gehrz et al. 1984) and QU Vul (Gehrz et al. 1986) displayed strong, optically thin 11.3 μm silicon carbide (SiC) and/or 10 and 20 μm silicate emission features. V842 Cen exhibited multiple hydrocarbon and 10 μm silicate emission features (see Gehrz 1990; Smith, Aitken, & Roche 1994). In QV Vul, four signature types of astrophysical dust were observed (Gehrz et al. 1992). Initially in QV Vul, an optically thick carbon dust continuum evolved through a period with superposed 3.2–3.4 μm hydrocarbon and 11.3 μm SiC features present. In a later phase, the continuua were dominated by optically thin 10 and 20 μm silicate emission. The case of QV Vul was quite intriguing, as it raised the possibility that different types of dust may have formed at different times in ejecta having large velocity and/or chemical gradients.

We observed V705 Cas through most of its major IR stages. Our earliest observations were obtained during the transition from an optically thick "pseudophotosphere" SED to that of free-free emission. Later observations followed the nova through dust formation, IR maximum, and the later stages of the dust shell evolution. Our series of IR photometric and spectroscopic measurements of V705 Cas permit determination of physical parameters (Table 1) associated with the ejecta as well as allowing a detailed study of an ejected shell containing a complex mixture of grain materials similar to those seen in the ejecta of QV Vul.

2. OBSERVATIONS

We obtained 1.2–18.5 μm IR photometric observations of V705 Cas on several occasions between 1993 December 14.1 UT (day 7.1) and 1996 June 23.4 UT (day 929.4). A summary of the entire photometric record is presented in Table 2. Data obtained during a five-day interval near day 373 have been averaged to produce a single data point to simplify the global analysis of the SED evolution (§ 3). On 1994 November 4 (day 343), an 8–13 μm ($R = \lambda/\Delta\lambda = 100$) spectrum of V705 Cas was obtained with the Cornell University SpectroCam-10 (SC-10) infrared spectrometer (Hayward et al. 1993). Details and preliminary analysis of the photometry and reduced spectrum were presented in Gehrz et al. (1995a).

3. GENERAL MORPHOLOGY OF THE INFRARED DEVELOPMENT OF V705 CASSIOPEIAE

Ney & Hatfield (1978) obtained a template, which is useful in studying the general temporal development of dust-forming novae, by monitoring NQ Vulpeculae 1976 for 235 days after outburst. They identified three distinct

[1] NSF Presidential Faculty Fellow.
[2] 1995 Ronald McNair Scholar, University of Wyoming.

TABLE 1

SUMMARY OF DERIVED PHYSICAL PARAMETERS

Parameter	Relationship	V705 Cassiopeiae
Day 0	Discovery date	JD 2,449,328.5
t_2	Visible light curve	64 days
t_3	Visible light curve	90 days
V_0	Spectra	840 km s^{-1}[a]
$(m_V)_{max}$	...	6.5
A_V	Color excess	1.6
$(M_V)_{max}$	Equation (2)	-7.0
D	Distance modulus	2.4 kpc
T_{IRmax}	Blackbody fit to data	690 K
$(\lambda F_\lambda)_{outburst}$	Visible light curve	2.3×10^{-14} W cm^{-2}
$(\lambda F_\lambda)_{IRmax}$	Observation	1.1×10^{-14} W cm^{-2}
$L_{outburst}$	...	$5.5 \times 10^4\ L_\odot$
L_{IRmax}	...	$2.5 \times 10^4\ L_\odot$
$L_{IRmax}/L_{outburst}$	...	0.5
τ_V	...	6
M_{gas}	Free-free emission (eq. [1e], day 7.1)	$\sim 10^{-5}\ M_\odot$
M_{carbon}	Equation (8)	$6.0 \times 10^{-7} M_\odot$
$M_{silicates}$	Equation (7)	$\sim 7.0 \times 10^{-8} M_\odot$
M_{carbon}/M_{gas}	...	~ 0.1
$M_{silicates}/M_{gas}$	...	$\sim 7.0 \times 10^{-3}$

[a] Woodward & Greenhouse 1993.

phases in the shell evolution. Immediately following the outburst, an expanding pseudophotosphere was visible as the optically thick ejecta moved outward. As the expanding shell became optically thin, a free-free emission phase was observed. The third phase began at the onset of dust formation. All three of the stages described by Ney & Hatfield (1978) in part were observed in V705 Cas. Figure 1 illustrates the phase relationships among several important parameters that describe the development of the nova shell.

Day 7.1 and 8.1 observations (Fig. 2*a*) showed the nova in transition from the pseudophotospheric to the free-free emission stage. At this epoch, the SED retained the characteristic psuedophotospheric blackbody form at wavelengths shorter than 3.8 μm. Beyond 3.8 μm, the SED exhibited the profile of 10^4 K free-free emission. By day 57.9 (Kidger et al. 1994), the SED had completely evolved into the free-free emission stage. Observations of other novae have shown that within a couple weeks after outburst, the pseudophotosphere fades away and the IR SED is dominated by free-free emission (Gehrz 1988). Therefore, it is likely that the free-free stage was reached well before day 57.9.

The dust formation stage likely commenced $\sim$70 days after outburst. Near this epoch, the observed visible magnitude of V705 Cas started a steep decline (see Gehrz et al. 1995a, Fig. 1). A sharp decrease in the visible magnitude is often one of the first clues that dust has condensed from the ejecta. Day 70.9 observations (Fig. 2*b*) can be fitted to a $\sim$1175 K blackbody SED, which we attribute to amorphous carbon dust emission. Most dust-forming novae have been observed to form carbon grains (Gehrz et al. 1995b), which results in a smooth IR SED. Maximum dust shell development occurred around day 105 with an optical depth of $\tau_V \sim 6$. By this time, the nova had fallen into a deep visual minimum ($m_V \sim +16$).

Since we were able to observe V705 Cas over 2.5 yr after outburst, we obtained data well beyond the initial dust formation stage. Figure 2*c* shows the post-IR maximum evolution of the ejecta. On day 105.9, the nova still retained the characteristic carbon SED. By day 136.8, the SED had evolved into a more complex form. At short wavelengths ($\lambda \leq 5$ μm), the SED continued to be dominated by carbon

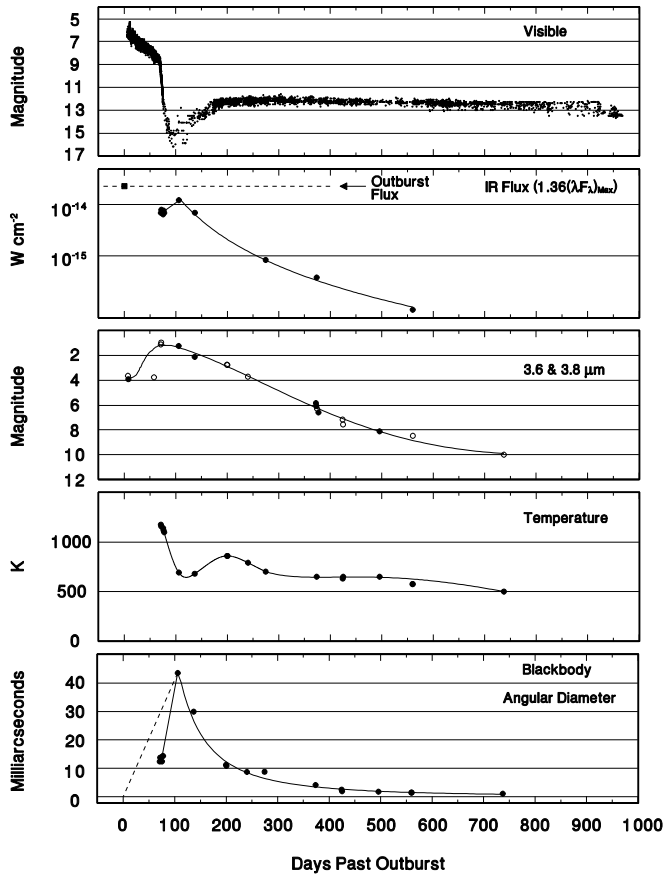

FIG. 1.—Temporal development of V705 Cassiopeiae showing the phase relationships among several crucial parameters. Maximum dust shell emission occurred during the visual transition phase. IR brightening (3.6 and 3.8 μm) occurred as the visible flux entered the transition phase. One-half of the outburst luminosity was eventually reradiated by the dust shell. Visual magnitudes are from the American Association of Variable Star Observers (J. A. Mattei 1996, private communication). For the 3.6 and 3.8 μm frame, filled circles correspond to the 3.6 μm data, and the open circles correspond to the 3.8 μm data.

TABLE 2

INFRARED MAGNITUDES OF V705 CASSIOPEIAE

Day [a]	1.6 μm			3.6 μm	3.8 μm	4.9 μm							
	J	*H*	*K*	*L*	*L*	*M*	7.8 μm	8.7 μm	9.8 μm	10.3 μm	11.6 μm	12.5 μm	18.5 μm
7.1[b]	4.82 ± .03	4.48 ± 0.03	4.18 ± 0.03	...	3.65 ± 0.03	3.00 ± 0.03	...	...	...	...	...	...	...
8.1[c]	...	4.55 ± 0.03	4.12 ± 0.03	3.92 ± 0.03	...	...	...	...	...	...	...	...	...
57.9[e]	6.37 ± 0.03	6.04 ± 0.03	5.43 ± 0.03	...	3.77 ± 0.03	...	...	...	...	...	...	...	...
70.9[e]	6.64 ± 0.03	4.80 ± 0.03	3.13 ± 0.03	...	1.11 ± 0.03	...	...	...	...	...	...	...	...
71.8[e]	6.55 ± 0.03	4.68 ± 0.03	2.98 ± 0.03	...	0.96 ± 0.03	...	...	...	...	...	...	...	...
75.1[f]	7.02 ± 0.05	4.99 ± 0.05	3.22 ± 0.05	...	...	...	...	...	...	...	...	...	...
76.1[f]	7.00 ± 0.10	4.80 ± 0.10	3.10 ± 0.10	...	...	...	...	...	...	...	...	...	...
77.1[f]	7.18 ± 0.03	4.93 ± 0.03	3.19 ± 0.03	...	...	...	...	...	...	...	...	...	...
105.9[c] ...	...	...	4.60 ± 0.16	1.23 ± 0.02	...	−0.06 ± 0.01	...	−1.16 ± 0.19	−1.28 ± 0.17	−0.82 ± 0.31	...	...	...
136.8[c] ...	...	...	5.19 ± 0.17	2.11 ± 0.03	...	0.68 ± 0.15	−0.71 ± 0.05	−0.99 ± 0.20	−1.20 ± 0.10	−0.84 ± 0.10	−1.04 ± 0.05	−1.22 ± 0.10	...
199.4[b] ...	10.53 ± 0.04	8.04 ± 0.03	5.66 ± 0.03	...	2.75 ± 0.03	1.95 ± 0.03	...	...	...	...	...	...	...
200.4[b] ...	10.49 ± 0.02	8.08 ± 0.02	5.66 ± 0.03	...	2.77 ± 0.02	...	...	...	...	...	...	...	...
240.2[b] ...	10.41 ± 0.03	9.06 ± 0.02	6.75 ± 0.02	...	3.72 ± 0.04	...	...	...	...	...	...	...	...
274.5[d] ...	...	...	7.50 ± 0.02	4.51 ± 0.04	...	3.34 ± 0.01	1.73 ± 0.01	1.07 ± 0.05	1.02 ± 0.04	0.99 ± 0.04	0.97 ± 0.16	0.91 ± 0.03	...
372.3[c] ...	...	...	...	5.86 ± 0.05	...	4.88 ± 0.16	2.01 ± 0.07	1.59 ± 0.06	1.44 ± 0.07	1.52 ± 0.10	1.25 ± 0.07	1.62 ± 0.13	0.41 ± 0.26
373.0[c] ...	...	...	...	6.09 ± 0.05	...	5.12 ± 0.08	2.48 ± 0.08	1.95 ± 0.03	1.68 ± 0.07	1.68 ± 0.06	1.68 ± 0.06	1.95 ± 0.15	1.19 ± 0.24
373.5[g] ...	12.59 ± 0.22	11.28 ± 0.01	8.97 ± 0.20	6.18 ± 0.07	...	5.04 ± 0.08	2.04 ± 0.11	1.65 ± 0.08	1.44 ± 0.08	1.44 ± 0.08	1.31 ± 0.08	1.70 ± 0.08	0.77 ± 0.12
374.5[b] ...	12.59 ± 0.22	11.28 ± 0.01	9.42 ± 0.03	...	6.32 ± 0.09	5.36 ± 0.09	...	...	...	...	...	...	...
377.1[c] ...	...	...	9.37 ± 0.23	6.61 ± 0.05	...	4.96 ± 0.07	2.39 ± 0.05	1.96 ± 0.07	1.76 ± 0.05	1.62 ± 0.05	1.50 ± 0.06	1.95 ± 0.09	0.82 ± 0.10
424.1[b] ...	12.60 ± 0.03	11.60 ± 0.02	9.95 ± 0.01	...	7.19 ± 0.05	...	...	...	...	...	...	...	...
425.1[b] ...	12.63 ± 0.05	11.74 ± 0.03	10.13 ± 0.03	...	7.58 ± 0.16	...	...	...	...	...	...	...	...
495.9[c] ...	...	...	...	8.14 ± 0.24	...	...	3.62 ± 0.16	3.33 ± 0.15	2.59 ± 0.20	2.82 ± 0.17	3.25 ± 0.29	...	...
559.5[c] ...	...	...	...	...	...	...	...	3.39 ± 0.31	2.96 ± 0.26	2.44 ± 0.16	2.67 ± 0.22	2.12 ± 0.21	...
560.5[b] ...	12.96 ± 0.09	12.49 ± 0.05	11.30 ± 0.03	...	8.50 ± 0.10	...	...	...	...	...	...	...	...
737.2[b] ...	13.59 ± 0.07	13.17 ± 0.03	12.46 ± 0.11	...	10.02 ± 0.26	...	...	...	...	...	...	...	...
905.4[b] ...	14.00 ± 0.09	13.78 ± 0.06	13.31 ± 0.10	...	...	...	...	...	...	...	...	...	...
929.4[b] ...	13.84 ± 0.04	13.67 ± 0.03	12.97 ± 0.06	...	...	...	...	...	...	...	...	...	...

[a] Days past outburst (JD 2,449,328.5).
[b] University of Minnesota InSb; $J = 1.25$ μm, $K = 2.2$ μm.
[c] University of Minnesota Bolometer; $J = 1.2$ μm, $K = 2.3$ μm
[d] Infrared Telescope Facility Bolometer; $K = 2.3$ μm.
[e] Kidger et al. 1994.
[f] Garnavich et al. 1994.
[g] Average of days 372.3, 373.0, 374.5, and 377.1.

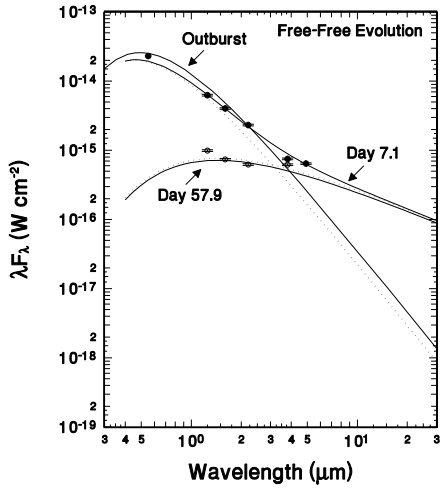

FIG. 2*a*

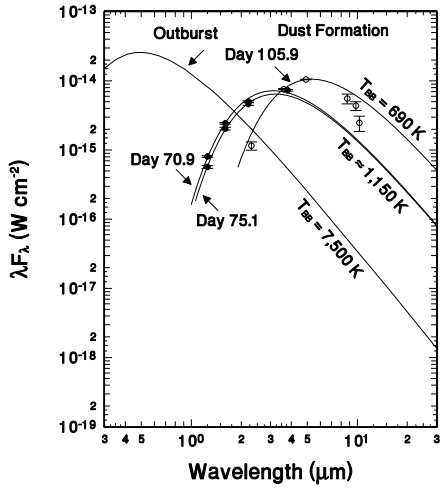

FIG. 2*b*

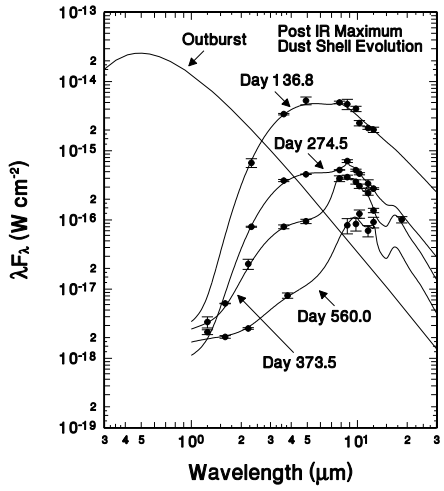

FIG. 2*c*

FIG. 2.—IR temporal development of V705 Cassiopeiae spanning from 1993 December 14.1 to 1996 June 23.4. At outburst, the SED was similar to that of an F star. (*a*) The SED evolved from an optically thick pseudo-photosphere to that of free-free emission. (*b*) About 70 days past outburst, carbon dust formed in the nova's ejecta. Amorphous carbon dust produces a featureless Planckian-type SED. Dust emission peaked about day 105. (*c*) As the carbon dust cooled and dispersed, emission features from hydrocarbon and silicate dusts were observed. These types of dust are responsible for the non-Planckian SED at longer wavelengths.

emission. However, it is apparent that at long wavelengths ($\lambda \geq 5$ μm), emission from components other than amorphous carbon grains are required. As the shell evolved past day 136.8, distortion of the SED from a simple carbon blackbody increased. After day 560.5, the nova was too dim to measure beyond 5 μm, and we were unable to follow the long-wavelength evolution beyond this epoch.

4. MODELING OF THE SED OF V705 CASSIOPEIAE

In order to account for the curious SED displayed beyond 5 μm, we found it necessary to employ a combination of emission (see Figs. 2 and 3*a*; eq. [1a]) from carbon (eq. [1b]), hydrocarbon (eq. [1c]), and silicate (eq. [1d]) dust grains. Free-free emission (eq. [1e]; Allen 1973) is necessary to model the shorter wavelength data prior to dust condensation and beyond day 274.5.

$$(\lambda F_\lambda)_{\rm total} = (\lambda F_\lambda)_{\rm carbon} + (\lambda F_\lambda)_{\rm hydrocarbon} + (\lambda F_\lambda)_{\rm silicate} + (\lambda F_\lambda)_{\rm free-free}\,, \tag{1a}$$

$$(\lambda F_\lambda)_{\rm carbon} = \epsilon(\lambda)_{\rm carbon}\,\frac{0.037R^2}{D^2}\,\frac{1}{\lambda^4}\,\frac{1}{[\exp\,(14388/\lambda T)] - 1}\,, \tag{1b}$$

$$(\lambda F_\lambda)_{\rm hydrocarbon} = \frac{R^3}{D^2}\sum_i \frac{\lambda(C_i N_i)}{[(\lambda - \lambda_{0_i})^2 + \gamma_i^2/4]}\,, \tag{1c}$$

$$(\lambda F_\lambda)_{\rm silicate} = \epsilon(\lambda)_{\rm silicate}\,\frac{0.037R^2}{D^2}\,\frac{1}{\lambda^4}\,\frac{1}{[\exp\,(14388/\lambda T)] - 1}\,, \tag{1d}$$

$$(\lambda F_\lambda)_{\rm free-free} = 2.11 \times 10^{-18} N_e^2\, T^{-1/2}\lambda^{-1} \times R^3 D^{-2} \exp\,(-14388/\lambda T)\,. \tag{1e}$$

In equations (1a)–(1e), the flux, λF_λ, is in watts per square centimeter, the wavelength, λ, is in microns, the ejected shell radius, R, is in parsecs, the distance to V705 Cas, D, is in kiloparsecs, and the temperature, T, is in kelvins. For equations (1b) and (1d), $\epsilon(\lambda)$ is the emissivity function for carbon and silicates, respectively. The carbon components are modeled using both optically thin and thick (at 1–20 μm) shells. The optically thick shells are modeled using the Planck function. The optically thin shells are modeled using the Planck function modified by a λ^{-1} emissivity function (Smith et al. 1994). The decision of whether to use an optically thick or thin shell was dictated by the quality of the fit to the photometry. An optically thick shell is used for observations up to day 274.5. An optically thin shell is used for observations from day 373.5 on. The silicate feature is modeled using the Planck function modified by the emissivity function for pure 0.3 μm spherical olivine ($MgFeSiO_4$) grains derived from absorption coefficients calculated by J. Sarmecanic (1996, private communication). Silicate grains younger than a few hundred days are unlikely to have experienced significant ultraviolet (UV) processing or to have formed mantles. Therefore, it is expected that silicates found in young novae ejecta should be, in general, very pure (Smith et al. 1994). For this reason, we use the absorption coefficients for pure olivine rather than those derived for "astronomical" silicates (see, e.g., Draine & Lee 1984). Pure silicates have been found to provide better fits to observation than astronomical silicates for several novae including Aql 1982, Cen 1986, and Her 1991 (Smith et al. 1994).

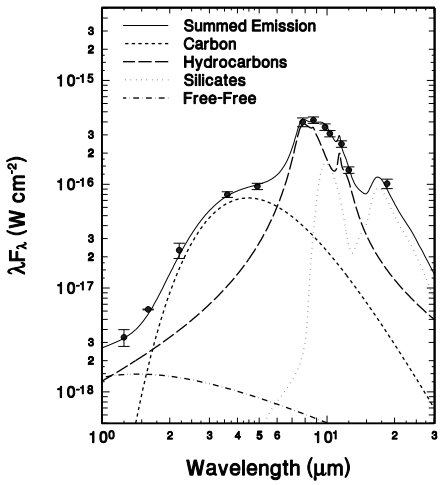

FIG. 3a

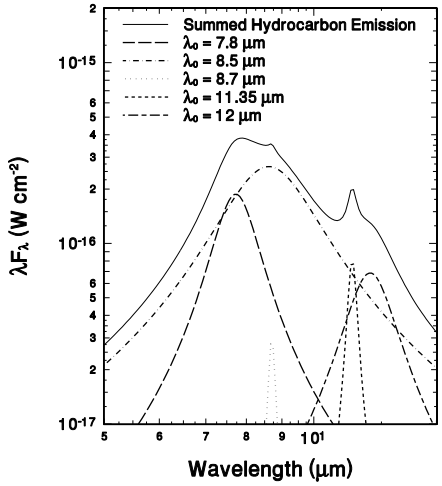

FIG. 3b

FIG. 3.—(a) Day 373.5 1.2–18.5 μm photometry. Amorphous carbon (*short dashed curve*), hydrocarbon (*long dashed curve*), silicate (*filled circles*), and free-free (*dot-dashed curve*) emission combine to fit observations. (*b*) The hydrocarbon feature is comprised of major emission components at 7.7 and 8.7 μm and broad emission components centered at 8.5 and 12.0 μm.

Hydrocarbon emission is modeled using a combination of major, minor, and broad emission features. Each feature is modeled using Lorentzian resonances (Smith et al. 1994; Allamandola, Thielens, & Barker 1989) with central wavelengths (λ_{0_i}) and FWHMs (γ_i) from Allamandola et al. (1989). We present the central wavelengths and FWHMs of the modeled hydrocarbon features in Table 3 and Figure 3*b*. In equation (1c), N_i is the density of molecules emitting in band *i*. C_i is a normalization constant. The model values for ($C_i N_i$) are given in Table 4.

TABLE 3

HYDROCARBON EMISSION MODELING PARAMETERS

λ_0	γ	Feature
Major Bands		
7.7	1.18	...
8.7	0.23	...
11.35.....	0.38	...
Minor Band		
12.7	0.48	...
Broad Bands		
8.5	2.78	5.52–9.52
12.0	2.07	10.5–13.5

NOTE.—All values are given in microns (see Allamandola et al. 1989).

The carbon dust shell evolution of V705 Cas was similar to that observed in most other dust-forming novae (Gehrz 1995). The dust shell formed $\sim$70 days after outburst and remained optically thick in the visible throughout our observations. Our initial observation of the carbon shell on day 70.9 yielded a dust temperature of $\sim$1175 K, which is well within the 1000–1200 K carbon dust grain condensation temperature commonly observed in novae. By day 105.9, the temperature had decreased to $\sim$690 K. Rather than continuing to decrease, the temperature rose to $\sim$860 K by day 199.4. The increase in grain temperature suggests that the grains decreased in size as the shell evolved past IR maximum (see § 5.5). After day 200.4, the temperature resumed a steady decrease. Our final measurement of the carbon shell on day 737.2 gave a temperature of $\sim$500 K.

Hydrocarbons are responsible for two prominent complexes of IR emission features: one from $\sim$3.2–3.7 μm and the other from $\sim$6–14 μm. Each complex is a collection of several major, minor, and broad emission components (Allamandola et al. 1989). In this paper, we focus primarily on the longer wavelength features. The 3 μm features in V705 Cas are discussed in Gehrz et al. (1995a) and Woodward et al. (1998). To interpret our mid-IR observations, we model the longer wavelength hydrocarbon emission using a combination of major emission bands at 7.7, 8.7, and 11.35 μm, a minor band at 12.7 μm, and broad features centered at 8.5 and 12.0 μm (Table 3). An example of how the separate emission bands are combined to form the complete hydrocarbon feature is shown in Figure 3*b*. Day 136.8 photometry revealed the first evidence for hydro-

TABLE 4

HYDROCARBON MODELING CONSTANTS ($C_i N_i$) [a]

Day	7.7 μm	8.5 μm	8.7 μm	11.35 μm	12.0 μm	12.7 μm
136.8.....	5.2×10^{-6}	2.6×10^{-5}	1.7×10^{-8}	0	7.0×10^{-7}	0
274.5.....	0	1.3×10^{-6}	4.3×10^{-9}	0	1.3×10^{-7}	0
373.5.....	7.3×10^{-8}	5.1×10^{-7}	3.8×10^{-10}	2.2×10^{-9}	5.2×10^{-8}	0
560.0.....	7.6×10^{-9}	3.8×10^{-8}	2.5×10^{-11}	0	1.1×10^{-8}	3.0×10^{-10}

[a] $C_i N_i$ is in watts per square centimeter.

carbon emission in the ejecta. The feature was observed as a flux excess above the smooth carbon SED from ~7–13 μm in narrowband filters. Similar features were observed in photometry from days 274.5, 373.5, 495.9, and 560.5 and in the 8–13 μm SC-10 spectrum from day 343, well after IR maximum. The observations support the contention of Evans & Rawlings (1994) that hydrocarbon emission does not occur until after visible recovery.

Figure 3 shows the day 343 SC-10 spectrum and day 373.5 photometry along with the model fit to the data. The model fit is a combination of carbon, hydrocarbon, and silicate emission, with hydrocarbon and silicate emission being the most prominent. In general, the marked 11.35 μm feature would be expected to be observed at 11.2 μm. Hydrocarbon emission features are due to UV excitation of vibrational modes in carbon—hydrogen and carbon —carbon bonds (Allamandola et al. 1989). The shift in wavelength observed at 11.2 μm is most likely caused by anharmonicity in C—H vibrational modes. The effect of the anharmonicity is to broaden and shift emission bands toward longer wavelengths (Barker, Allamandola, & Thielens 1987) when the molecule is excited to higher vibrational modes. Since nova ejecta are subject to intense UV radiation from a hot WD, the wavelength shift is expected. We observed the long wavelength hydrocarbon features until day 560. Beyond this epoch, the features were too dim to detect. Our model suggests that the long-wavelength hydrocarbon emission flux decreased by about a factor of 10 over the span of our observations.

The long-wavelength excess cannot be accounted for from hydrocarbon emission alone. We introduce a silicate emission component to account for the remainder of the flux observed in the 9.8 and 18.5 μm broadband filters. Silicates possess two strong features in the IR. There is a broad feature centered at 9.7 μm and a narrower band centered at 18 μm. Our first observation of silicate emission occurred on day 136.8 at 9.8 μm. Even though the 7–13 μm region of the SED was dominated by hydrocarbon emission at this time, a contribution from the 9.7 μm silicate band is required to fit the photometry. In later observations, as the hydrocarbon flux decreased, silicate emission became more apparent. On day 373.5, we observed the 18 μm feature (Fig. 3*a*). Detection of this feature further supports our contention that silicates were contained in the ejecta. Unfortunately, the temperature of the silicates is difficult to constrain owing to the large number of free parameters used to fit the SEDs. The best-fit estimate to the observational data suggests a silicate grain temperature of ~300–400 K. In other novae, silicates within this temperature range have been observed, with little temperature fluxuation as the ejecta temporally evolved (Smith et al. 1994). Figure 4 shows how carbon, hydrocarbon, and silicate emission combine to fit day 373.5 observations.

Another prominent IR feature occasionally observed in the spectrum of nova ejecta is the 11.3 μm SiC emission band (Gehrz 1988). SiC emission produces a relatively wide feature, FWHM ~ 1.4 μm (Goebel, Cheeseman, & Gerbault), and is often cited as the origin of the excess observed in the 10.3 and 11.6 μm narrowband photometry filters (Gilman 1974a). On several days, we observed flux in excess of the carbon continuum in these filters. However, our detection of an 18 μm feature on day 373.5 suggests that the 10.3 and 11.6 μm excesses are due to silicates rather than SiC. An obvious 11.3 μm emission feature was observed in

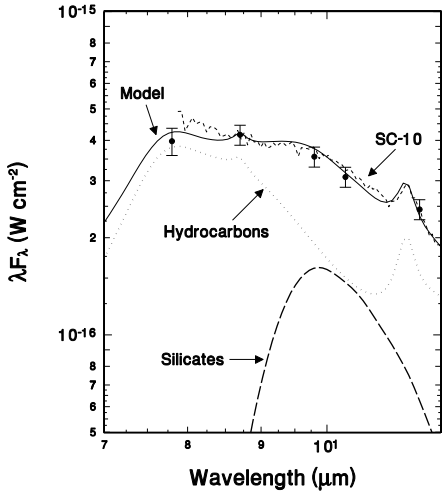

FIG. 4.—Day 373.5 photometry along with the day 343 SC-10 spectrum (*short dashed curve*) is fitted to emission from a combination of hydrocarbon, amorphous carbon, and silicate dust. The silicate (*long dashed curve*) and hydrocarbon (*filled circles*) components are shown. The amorphous carbon component lies below the limit of the plot.

the SC-10 spectrum. Once again, we attribute this feature to hydrocarbons rather than SiC. The SiC emission feature is about 3 times the width of the hydrocarbon feature. SiC emission produces too broad a feature to fit the observations. The 11.3 μm feature is modeled more accurately using hydrocarbon emission. In addition, the flux at wavelengths other than 11.3 μm must be accounted for. Our modeling shows this flux is likely attributed to hydrocarbon emission at 7.8, 8.5, 12, and 12.7 μm. In addition, 3 μm hydrocarbon flux was observed on several occasions by Gehrz et al. (1995a) and Woodward et al. (1998). It seems likely that the 11.3 μm feature also is due to hydrocarbons. In contrast, there is little observational evidence for the presence of SiC in the ejecta of V705 Cas.

5. PHYSICAL PARAMETERS OF THE CIRCUMSTELLAR SHELL OF V705 CASSIOPEIAE

5.1. *Distance and Luminosity*

A distance to V705 Cas can be calculated from the M_V-t_2 relationship (maximum magnitude rate of decline relationship), where t_2 is the time in days required for the nova to decrease 2 mag from visual maximum. Della Valle & Livio (1995) showed the relationship between M_V and t_2 to be

$$M_V = -7.92 - 0.81 \arctan\left(\frac{1.32 - \log t_2}{0.23}\right), \qquad (2)$$

where the value of arctan is in radians. Utilizing the visible light curve (Fig. 1), we find $t_2 = 64$ days and $(m_V)_{\max} = +6.5$. From t_2, we calculate an absolute visual magnitude from equation (2) of $M_V = -7.0$. By applying 1.6 mag of visual extinction (Hauschildt et al. 1994), we estimate a distance of ~2.4 kpc to V705 Cas. Utilizing this distance, an outburst luminosity in $L_\odot$ is calculated from

$$L_{\text{outburst}} = 4.18 \times 10^{17} D^2 (\lambda F_\lambda)_{\text{outburst}}, \qquad (3)$$

where D is the distance to V705 Cas in kiloparsecs and $(\lambda F_\lambda)_{\text{outburst}}$ is the maximum emission from the pseudophotosphere blackbody spectrum in watts per sqaure centimeter. At 0.55 μm, $(\lambda F_\lambda)_{\text{outburst}} = 2.3 \times 10^{-14}$ watts per

square centimeter, resulting in a luminosity of $5.5 \times 10^4\ L_\odot$. This is in excess of the Eddington luminosity for a solar mass progenitor ($L_{\rm Edd} = 5 \times 10^4\ L_\odot$).

5.2. *Mass of the Gas Expelled in the Nova Outburst*

The gas number density is calculated from λF_λ, and the flux due to free-free emission is calculated from equation (1e). On day 7.1, we measured a free-free flux of 2.6×10^{-16} W cm^{-2} at 10 μm. An expansion velocity of 840 km s^{-1} (Woodward & Greenhouse 1993) and a temperature of 10^4 K results in an electron density of 1.3×10^{10} cm^{-3}. Assuming the gas ejecta are composed entirely of hydrogen, and the contents fill a sphere of radius R, $M_{\rm gas} = 6.3 \times 10^{-6}\ M_\odot$. Models of CO novae have shown that the initial shock ejection of gas likely lasts on the order of 10 days (Prialnik 1986). Therefore, we assume an initial, steady rate of ejection for the first 10 days. From day 7.1, we calculate an ejection rate of $\dot{M}_0 = 2.3 \times 10^{22}$ g s^{-1}. This rate is comparable to rates calculated for other novae (Prialnik 1986; Shara 1981). Assuming the initial shock ejection is followed by a wind with a mass loss rate of

$$\dot{M}_{\rm gas} = \dot{M}_0\, t^{-2} \tag{4}$$

(Kwok 1983) and mass loss is finished within the t_3 time (Livio 1996; Shara 1981), a total gas mass can be estimated. Integrating equation (4) from day 10 to day 90 (t_3 time), we calculate an ejected gas mass of $M_{\rm gas} \sim 10^{-5}\ M_\odot$. We use this mass as a rough estimate of the total mass of gas ejected from the nova.

5.3. *Total Mass of Carbon Grains Expelled in the Nova Outburst*

The IR luminosity of a shell composed of N spherical grains of radius a and temperature $T_{\rm BB}$ is given by

$$L_{\rm IR} = N 4\pi a^2 Q_e \sigma T_{\rm BB}^4\ , \tag{5}$$

where Q_e is the Planck mean emission cross section for a grain, and σ is the Stefan-Boltzmann constant. The total dust grain mass in the shell is

$$M_{\rm dust} = N\left(\frac{4\pi}{3}\right)\rho a^3\ , \tag{6}$$

where ρ is the density of the condensed material. Combining equations (5) and (6) yields the expression

$$M_{\rm dust} = 1.15 \rho a L_{\rm IR}\, Q_e^{-1}\, T_{\rm BB}^{-4}\ , \tag{7}$$

where $M_{\rm dust}$ is given in solar mass, ρ in grams per centimeter cubed, $L_{\rm IRmax}$ in solar luminosity, and $T_{\rm BB}$ in kelvins.

For a shell composed of carbon grains for which $a \leq 1$ μm and $T_{\rm BB} \leq 1000$ K, $Q_e = 0.01 a T_{\rm BB}^2$ (Gilman 1974b). Equation (7) may be combined along with the above expression for Q_e to yield the expression

$$M_{\rm carbon} = 1.15 \times 10^6 \rho L_{\rm IRmax}\, T_{\rm BB}^{-6}\ . \tag{8}$$

At IR maximum ($\sim$day 105.9), the luminosity was 2.5×10^4 $L_\odot$ and $T_{\rm BB} \sim 690$ K. The density of condensed carbon is 2.25 g cm^{-3}, yielding $M_{\rm carbon} = 6.0 \times 10^{-7}\ M_\odot$. Assuming the gas ejecta are composed entirely of hydrogen, the carbon-to-gas mass ratio is $\sim$0.1. This results in a carbon mass overabundance of $\sim$20 relative to solar.

5.4. *Abundance of Silicate Dust in the Ejecta*

There is likely considerable uncertainty regarding the modeling of the silicate features. This uncertainty is due to the difficulty of fitting a large number of parameters (i.e., several hydrocarbon features, the carbon continuum, and silicate emission) to the ($R \sim 10$) photometry. Therefore, we estimate the mass of silicates in the ejecta by averaging the masses calculated (eq. [7]) from our five observations when silicate emission was observed. Using the olivine absorption coefficients from J. Sarmecanic (1996, private communication), we calculate $Q_e \sim 0.1$ for 300–400 K 0.3 μm silicate grains. A silicate mass density of 3 gm cm^{-3} results in a silicate dust mass of $M_{\rm silicate} \sim 7 \times 10^{-8}\ M_\odot$. Once again, assuming the gas ejecta are composed entirely of hydrogen, the silicate-to-gas mass ratio is $\sim 7 \times 10^{-3}$. Therefore, those elements that compose the silicates, O, Mg, Fe, and Si, exist as solids in roughly solar abundance.

5.5. *Post-IR Maximum Development of the Dust Grains*

The post-IR maximum increase in grain temperature was accompanied by a rapid decrease in angular diameter of the dust grains inferred from the carbon blackbody SED (Figs. 2*a–c*). The decline in $(\lambda F_\lambda)_{\rm max}$ after day 105.9 suggests that grain growth in the shell of V705 Cas was completed by this date. Graphite grains of radius a, whose Planck mean cross section is $Q_e = 10^{-2} a T_{\rm BB}^2$, will cool as they flow away from the central star as

$$T_{\rm BB} = 2.3 \times 10^6 \left(\frac{L}{a}\right)^{1/6} \left(\frac{1}{R}\right)^{1/3} \propto t^{-1/3}\ , \tag{9}$$

where L is the luminosity of the embedded source in $L_\odot$, and a and R are in centimeters. If a and L remain constant, the cooling rate as a function of time goes as $t^{-1/3}$.

The blackbody angular diameter in milliarcseconds for grains with $Q_e = 10^{-2} a T_{\rm BB}^2$ is

$$\Theta_{\rm BB} = 9.8 \times 10^{22} [(N a^3 L)/(R\, d\, T_{\rm BB})] \propto t^{-2/3}\ , \tag{10}$$

where N is the total number of grains in the shell, L is the luminosity of the embedded source in solar luminosity, and a, R, and d are in centimeters. For constant L, N, and a, $\Theta_{\rm BB}$ will decrease as $t^{-2/3}$. Figure 1 shows $\Theta_{\rm BB}$ decreased considerably faster than $t^{-2/3}$ following day 105.9. It is evident from equations (9) and (10) that only a reduction in the grain radius could have caused $T_{\rm BB}$ to rise after day 105.9, while at the same time causing $\Theta_{\rm BB}$ to decrease at such a rate. Clayton & Wickramasinghe (1976) have argued that N remains relatively constant after condensation has occurred. A reduction in N would not have affected $T_{\rm BB}$. Decreasing L would cause both $T_{\rm BB}$ and $\Theta_{\rm BB}$ to fall. Therefore, the grains must have decreased in size as the shell evolved past IR maximum. Mitchell, Evans, & Bode (1983) have suggested that grains likely decrease in size due to sputtering possibly caused by interaction with a high-velocity secondary ejecta. Grain temperature warming trends have been observed in the late stages of shell development of NQ Vul (Ney & Hatfield 1978) and LW Ser (Gehrz et al. 1980).

5.6. *Bolometric Evolution*

Novae are known to go through a period of constant bolometric luminosity that begins shortly after outburst and may continue for several years (see Krautter et al. 1996). For a dust-forming nova, a significant amount of energy radiated by the remnant WD may be absorbed and rera-

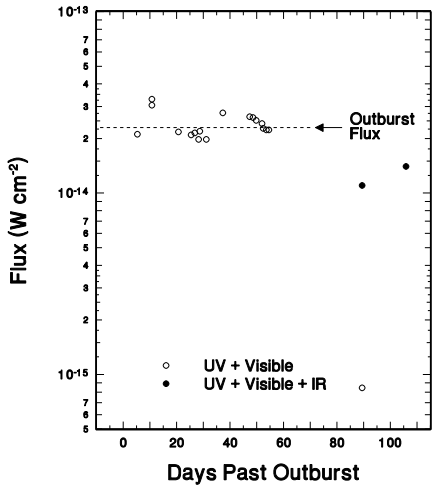

FIG. 5.—The bolometric flux of V705 Cassiopeiae. Prior to the visible transition, the flux was dominated by the visible and UV (data from Hauschildt et al. 1994). After transition, the flux was dominated by the IR.

diated in the IR. The ratio of maximum IR luminosity to the outburst luminosity ($L_{\rm IRmax}/L_{\rm outburst}$) measures the degree of coverage of the central engine by the dust shell. The central engine luminosity may decrease by one-half before entering a period of constant luminosity. Therefore, $L_{\rm IRmax}/L_{\rm outburst} = 0.5$–1.0 suggests complete coverage. All CO novae observed to this date with visual extinctions ≥ 2.5 mag have had luminosity ratios within this range (Gehrz 1995).

The bolometric luminosity for V705 Cas from near outburst until day 105.9 is shown in Figure 5. The transition in the visible light curve, caused by the formation of dust, occurred approximately 70 days past outburst. Subsequent to transition, the bolometric luminosity stayed nearly constant at outburst luminosity and was dominated by the visible and UV. By day 89.5, the summed visible and UV luminosity had plummeted by better than a factor of 25 (Hauschildt et al. 1994). However, the IR luminosity had increased significantly, raising the day 89.5 luminosity to roughly one-half the outburst luminosity. At IR maximum (day 105.9) the visible and UV luminosity should be negligible. Therefore, the bolometric luminosity should be dominated by the IR. At this epoch, $L_{\rm IR} = 2.5 \times 10^{-4}\ L_{\odot}$, once again about one-half the outburst luminosity. Therefore, $L_{\rm IRmax}/L_{\rm outburst} = 0.5$, which indicates likely complete coverage of the central engine by the dust shell.

6. CONCLUSIONS

V705 Cas is the latest of a growing list of novae that have produced a variety of dust grains in their ejecta. Our observations showed evidence of amorphous carbon, hydrocarbons, and silicate condensates. However, we found no conclusive evidence for SiC grains in the ejecta. Carbon dust was responsible for an optically thick dust shell that reached a maximum optical depth of $\tau_V \sim 6$ about 105 days (IR maximum) after outburst. At this time, one-half of the outburst luminosity was reradiated by the dust shell. As the carbon dust cooled and dispersed, emission from hydrocarbons and silicates started to dominate the SED. Signatures of all three dust types were evident in our final observation beyond 5 μm on day 560.

Based on observations, carbon and silicate mass abundances were calculated. We found the nova ejecta to be significantly overabundant in carbon relative to solar. Solid-phase elements such as O, Mg, Fe, and Si were found to be present in roughly solar abundance. Gehrz et al. (1995a) concluded that O, Mg, Fe, and Si were significantly overabundant. However, this conclusion was made assuming that the 7.8–12.6 μm flux excess over the carbon continuum was due to silicate emission alone. We have shown instead that this region of the SED can be interpreted as being due to emission from both silicates and hydrocarbons. Therefore, the amount of silicates in the ejecta could be much less than originally proposed.

We thank J. A. Mattei for providing us with the American Association of Variable Star Observers visual light curve of V705 Cassiopeiae and J. Sermacanic for allowing us to use his olivine absorption coefficients. In addition, we thank M. Bode, who refereed this paper, for his helpful comments and suggestions that materially improved the discussion. C. G. M. and R. D. G. thank A. Knutson for assistance with observations at the Mount Lemmon Observing Facility. The University of Minnesota IR Group is supported by the NSF, NASA, Department of Defense, and the University of Minnesota Graduate School. C. E. W. and J. B. S. acknowledge support from the NSF (AST 94-53354, AST 95-26486) and the Office of Student Educational Opportunity, University of Wyoming.

REFERENCES

Allamandola, L. J., Thielens, A. G., & Barker, J. R. 1989, ApJS, 71, 733
Allen, C. W. 1973, Astrophysical Quantities (3d ed.; London: Athlone)
Barker, J. R., Allamandola, L. J., & Thielens, A. G. 1987, ApJ, 315, L61
Bode, M. F., Evans, A., Whittet, D. C. B., Aitken, D. K., Roche, P. F., & Whitmore, B. 1984, MNRAS, 207, 897
Bode, M. F., & Evans, A. 1989, Classical Novae, ed. M. F. Bode & A. Evans (London: John Wiley and Sons Ltd.), 163
Clayton, D. D., & Wickramasinghe, N. C. 1976, Ap&SS, 42, 463
Della Valle, M. & Livio, M. 1995, ApJ, 452, 704
Draine, B. T., & Lee, H. M. 1984, ApJ, 285, 89
Evans, A., & Rawlings, J. M. C. 1994, MNRAS, 269, 427
Garnavich, P. 1994, IAU Circ. 5941
Gehrz, R. D. 1988, ARA&A, 26, 377
———. 1990, in Physics of Classical Novae, ed. A. Cassatella & R. Viotti (Berlin: Springer), 138
———. 1993, Ann. Isr. Phys. Soc., 10, 100
———. 1995, in Proc. Abano-Terme Conference on Cataclysmic Variables, ed. M. Della Valle (Dordrecht: Kluwer), 29
Gehrz, R. D., Grasdalen, G. L., Greenhouse, M., Hackwell, J. A., Hayward, T., & Bently, A. F. 1986, ApJ, 308, L63
Gehrz, R. D., Grasdalen, G. L., Hackwell, J. A., & Ney, E. P. 1980, ApJ, 237, 855
Gehrz, R. D., Greenhouse, M. A., Hayward, T. L., Houck, J. R., Mason, C. G., & Woodward, C. E. 1995a, ApJ, 448, L119
Gehrz, R. D., Jones, T. J., Matthews, K., Neugebauer, G., Woodward, C. E., Hayward, T. L., & Greenhouse, M. A. 1995b, A&A, 110, 325
Gehrz, R. D., Jones, T. J., Woodward, C. E., Greenhouse, M. A., Wagner, R. M., Harrison, T. E., Hayward, T., & Benson, J. 1992, ApJ, 400, 671
Gehrz, R. D., Ney, E. P., Grasdalen, G. L., Hackwell, J. A., & Thornson, H. A. 1984, ApJ, 281, 303
Gehrz, R. D., Truran, J. W., & Williams, R. E. 1991, Protostars and Planets III, ed. E. Levy & J. Lunine, (Tuscon: Univ. of Arizona Press), 75
Gilman, R. C. 1974a, ApJ, 188, 87
———. 1974b, ApJS, 268, 397
Goebel, J. H., Cheeseman, P., & Gerbault, F. 1995, ApJ, 449, 246
Hauschildt, P. H., Starrfield, S. G., Shore, S. N., Gonzalez-Riestra, R., Sonneborn, G., & Allard, F. 1994, AJ, 108, 1008
Hayward, T. L., Miles, J. W., Houck, J. R., Gull, G. E., & Schoenwald, J. 1993, Proc. SPIE, 1946, 334
Kanatsu, K. 1993, IAU Circ. 5902
Kidger, M., Devaney, K., Sahu, K., & López, S. 1994, IAU Circ. 5936
Krautter, J., Oegelman, H., Starrfield, S., Wichmann, R., & Pfeffermann, E. 1996, ApJ, 456, 788
Kwok, S. 1983, MNRAS, 202, 1149

Livio, M. 1996, in Proc. Extragalactic Distance Scale, ed. M. Livio, M. Donahue, & N. Panagia (Cambridge: Cambridge Univ. Press), 196
Mitchell, R. M., Evans, A., & Bode, M. F. 1983, MNRAS, 205, 1141
Ney, E. P., & Hatfield, B. F. 1978, ApJ, 219, L111
Payne-Gaposchkin, C. 1964, The Galactic Novae (New York: Dover)
Prialnik, D. 1986, ApJ, 310, 222
Shara, M. M. 1981, ApJ, 243, 926
Smith, C. H., Aitken, D. K., & Roche, F. P. 1994, MNRAS, 267, 225
Woodward, C. E., & Greenhouse, M. A. 1993, IAU Circ. 5910
Woodward, C. E., Smilowitz, J. B., Mason, C. G., Gehrz, R. D., & Greenhouse, M. A. 1998, in preparation